Numerical analysis of ultra-thin $MASnI_3$ based perovskite solar cell by SCAPS-1D

Al. A. Siddique[a], S. Bin Helal[b], M. I. Haque[b,*]
[a]*Department of Electrical and Electronic Engineering, East Delta University, Abdullah Al Noman Road, Noman Society, East Nasirabad, Khulshi, Chattogram 4209, Bangladesh*
[b]*Department of Electrical and Electronic Engineering, International Islamic University Chittagong, Kumira, Chittagong, Bangladesh*

Future solar cells are perovskite solar cells (PSC). Silicon based solar cells offer an unlimited source of clean energy. Even if perovskite PCE is currently not at its optimum, it has shown great potential for improvement. Numerical analysis of PSC is now more convenient using different simulation software which is a great way to experiment on PSC. In this study, a unique structure of PSC has been proposed, its key parameters like acceptor density, perovskite defect density, interface defect density, and thickness has been investigated to find out their impact on device performance. After optimization a high power conversion efficiency (PCE) 30.57%, open circuit voltage of 1.02 V, short circuit current of 34.68 (mA/Cm^2) and fill factor 86.21% respectively was obtained.

(Received December 20, 2023; Accepted April 2, 2024)

Keywords: Perovskite solar cell, Lead-free, SCAPS, High efficiency, Defect density, Temperature effect

1. Introduction

Lead free Perovskite solar cells have been getting great attention recently because of their good electrical and optoelectrical properties, high PCE (power conversion efficiency), and easy fabrication technique. Perovskite is a 3rd generation solar cell with a general formula of ABX_3, where A is an organic cation. B is a metal cation and X is a halogen anion [1]. Perovskite has high absorption coefficient excellent bipolar charge mobility, long carrier diffusion length, low exciton binding energy, low trap state density and tunable band gap [1,31,32,33,34]. methyl ammonium (MA) lead halide ($MAPbX_3$) show high PCE [2], which is the most desired characteristic of a commercial solar cell. Many countries are stepping away from lead-based solar cells and have strict laws against using lead. Using lead causes many problems as it is a very toxic material and harmful to humans, animals, and the environment [3]. Lead-based solar cells are not very reliable for long use as lead has stability issues [4,35,36,37,38]. So many materials like Sn (II), Bi (III), Ti (IV), Sb (III), Ge (II) have been tried as a supplement to lead [5]. Among those Sn-based halide PSC got the most attention because of its similar properties to lead halide Perovskite [5] Sn-based PSC has an ideal band gap of 1.3 ev, low-temperature solvability, long life, ferroelectricity and absorption capacity of a large spectrum of light [6]. High PCE makes it a great candidate to substitute lead. CdSe, TiO_2 and ZnO have been used as electron transport layer (ETL)[7][8]. TiO_2 is the most popular ETL, but it has its disadvantages. TiO_2 has a high fabrication temperature and low electron mobility [8]. CdSe does not have a proper manufacturing process and has low crystallinity. ZnO can be a good substitute for TiO_2 because it has low fabrication temperature, higher electron mobility, wide band gap, good optical transmittance, low toxicity, and can be easily synthesized by spin coating technique[8][39]. Cu_aBx_b is a relation between copper-based chalcogenide compounds (where X=S, Te, and B= Bi, Sb, Sn) which are being used as P-type material[9][10]. Among all those compound $CuSbS_2$ (copper antimony sulfide) stand out because of it's ideal optical band gap of 1.38 ev-1.66 ev, low cost, non-toxic earth-abundant material[11][40].Thus $CuSbS_2$ has great potential to be used as hole transport material (HTL) in

* Corresponding author: ismail07rueteeee@iiuc.ac.bd
https://doi.org/10.15251/JOR.2024.202.187

PSC. Solar cell capacitance simulator (SCAPS) has been used in this study. In SCAPS different operational parameters like thickness, defect density, acceptor density, and temperature can be tested to find out the optimum performance. This proposed device is eco-friendly and has high PCE which could be used to power rural areas and also high power consuming commercial areas. Along with long last ability, this device can work under high temperature.

2. Methodology

2.1. Theory

Simulation softwares are useful tool to study and experiment on different solar cells. Various parameters like acceptor density, defect density, thickness, work function can be calculated and varied to get the optimum performance. SCAPS-1D is a very useful tool to simulate various solar cells. SCAPS solves three main physical differential equations (I) electron continuity equation (II) hole continuity and (III) passion equation in steady state and solves them continuously till the convergence occurs.

$$\frac{dp_n}{dt} = G_p - \frac{Pn-Pno}{\tau p} + P_n\mu_p\frac{d\varepsilon}{dx} + \mu_p\varepsilon\frac{dp_n}{dx} + D_p\frac{d^2p_n}{dx^2} \quad (1)$$

$$\frac{dn_p}{dt} = Gp\frac{n_pP_{po}}{\tau n} + n_p\mu_n\varepsilon\frac{d\varepsilon}{dx}\mu_n\varepsilon\frac{dn_p}{dx}Dn\frac{d^2np}{dn^2} \quad (2)$$

$$\frac{d}{dx}(-\varepsilon(x)\frac{d\varphi}{dx}) = q[p(x) - n(x) + N_D^+(x) - N_A^-(x) + P_t(x) - n_{t(x)}] \quad (3)$$

where,

Symbol	Definition
D	denote diffusion coefficient
Ξ	Electric field
G	Generation rate
Ψ	Electrostatic potential
Q	Electron charge
τp	Hole lifetime
τn	Electron lifetime
μp	Electron mobility
μn	Hole mobility
n(+)x	Trapped electron concentration
n(x)	Free electron concentration
pt(x)	Trapped hole concentration
p(x)	Free hole concentration
ND+(x	Ionized donor
NA-(x)	Ionized acceptor

Maximum power P_{max} is a product of current density J_{mp} and voltage at maximum power point V_{mp}

$$P_{max} = J_{mp} \times V_{mp} \quad (4)$$

Fill factor (FF) is a ration between maximum power and the product of open circuit voltage (V_{oc}) and short circuit current (J_{sc})

$$FF = \frac{P_{max}}{V_{oc} \times J_{sc}} \quad (5)$$

The power conversion efficiency can be calculated by

$$PCE = \frac{P_{max}}{P_{in}} = \frac{J_{mp} \times V_{mp}}{P_{in}} = \frac{V_{oc} \times J_{sc} \times FF}{p_{in}} \quad (6)$$

2.2. Device configuration

This Study proposes a new structure of perovskite solar cell (FTO/ZnO/$MASnI_3$/$CuSbS_2$/Pt). ZnO is used as electron transport material (ETL), $MASnI_3$ is used as the absorber layer and $CuSbS_2$ is used as HTL. Also, SnO_2: F (FTO) is used as transparent conducting material and Pt is used as anode material. In a solar cell, the band alignment of each layer is important for smooth function and optimum efficiency as it governs light absorption, carrier generation, and charge transport.

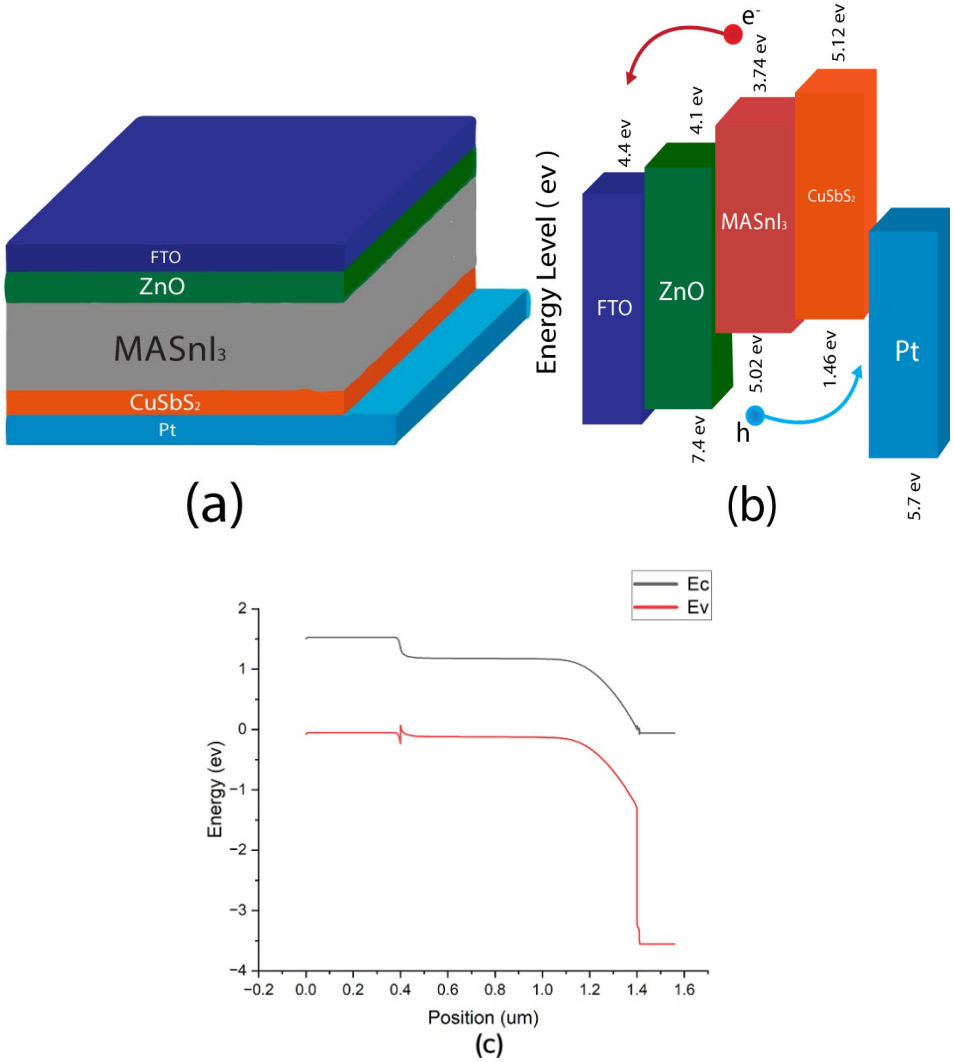

Fig. 1. (a) Schematic structure (b) Energy Band diagram (c) grading of energy parameters of simulated device.

2.3. Simulation parameters

All the values of different parameters used in this simulation are taken from various literatures, theories, and experiments. All basic parameters are listed in table 1 and defects parameters are listed in table 2.

Table 1. Basic parameters of each layer.[44-50]

Parameters	FTO (TCO)	ZnO (ETL)	$CH_3NH_3S_nI_3$ (absorber layer)	$CuSbS_2$ (HTL)
Thickness (nm)	100	10 variable	1000 variable	400 Variable
Bandgap energy, Eg (eV)	3.4	3.3	1.3	1.580
Electron affinity, χ (eV)	4.5	4.1	4.17	4.20
Relative permittivity, εr	9.1	9.0	8.2	14.60
Conduction band density of states, Nc (cm−3)	1.1×10^{19}	2.2×10^{18}	1×10^{18}	2×10^{18}
Valance band density of states, Nv (cm−3)	1.1×10^{19}	1.9×10^{19}	1×10^{18}	$1 \times^{19}$
Thermal velocity of electron and hole, (cm/s)	1×10^{7}	1×10^{7}	1×10^{7}	1×10^{7}
Electron mobility, μn (cm2 /Vs)	20	100	1.6	49
Hole mobility, μp (cm2 /Vs)	10	25	1.6	49
Donor concentration, ND (cm−3)	1.1×10^{19}	1×10^{18}	0	1×10^{15}
Acceptor concentration, NA (cm−3)	0	0	1×10^{16}	1.380 $\times 10^{18}$

Table 2. Defect parameters of each layers.[44-51]

Parameters	ZnO	$CH_3NH_3S_nI_3$	$CuSbS_2$	ZnO/ $CH_3NH_3S_nI_3$ Interface	$CH_3NH_3S_nI_3$ $CuSbS_2$ interface
Defect type	Neutral	Neutral	Neutral	Neutral	Neutral
σ_n (Cm^{-2})	1 $\times 10^{-15}$	1×10^{-15}	1×10^{-13}	1×10^{-15}	1×10^{-15}
σ_ρ (Cm^{-2})	1 $\times 10^{-15}$	1×10^{-15}	1×10^{-12}	1×10^{-15}	1×10^{-15}
Energy distribution	Single	Gaussian	Single	Single	Single
Characteristic energy (ev)	-	0.100	-	-	-
Energy level with respect to Ev (above Ev) (eV)	0.600	0.600	0.600	0.600	0.600
Defect density, Nt (cm−3)	1 $\times 10^{15}$	1×10^{14} (Variable)	1×10^{14}	1×10^{10}	1×10^{10}

3. Result and discussion

Simulation has been run for different values of perovskite thickness, ETL and HTL thickness, Acceptor doping density, perovskite defect density, Interface defect density and metal work function and obtained results are discussed below.

3.1. Optimization of thickness

Perovskite As the absorber layer plays an important role in device performance[12]. Thickness of the perovskite affects photovoltaic characteristics like V_{OC}, J_{SC}, FF ,and PCE [13,14]. In this study, the thickness of the absorber layer has been varied from 100nm-1000nm. As the thickness increases J_{SC} and PCE increases. PCE increases rapidly till 600nm. After 600nm, the increase in PCE was slow and the highest PCE 30.57% was recorded at 1000nm. As the thickness was increasing till a certain point, the absorber layer was still thin so a lot of photogenerated carrier could reach to electrode and generate power [15], so PCE was high. After 1000 nm PCE starts to drop with increase in absorber layer thickness because of higher recombination in thick absorber layer [15]. J_{SC} was continuously increasing because of significant absorption coefficient of perovskite [15]. Highest value of J_{SC} (34.842657 mA/Cm^2) was recorded at 1200 nm. V_{OC} and FF was decreasing with increase in absorber layer thickness. V_{OC} drops because of higher recombination of free charge carrier in thick absorber layer [13] and drop in FF was the result of increased series resistance [12,13]. Figure 2 shows the graphical representation of photovoltaic output as a function of absorber layer thickness.

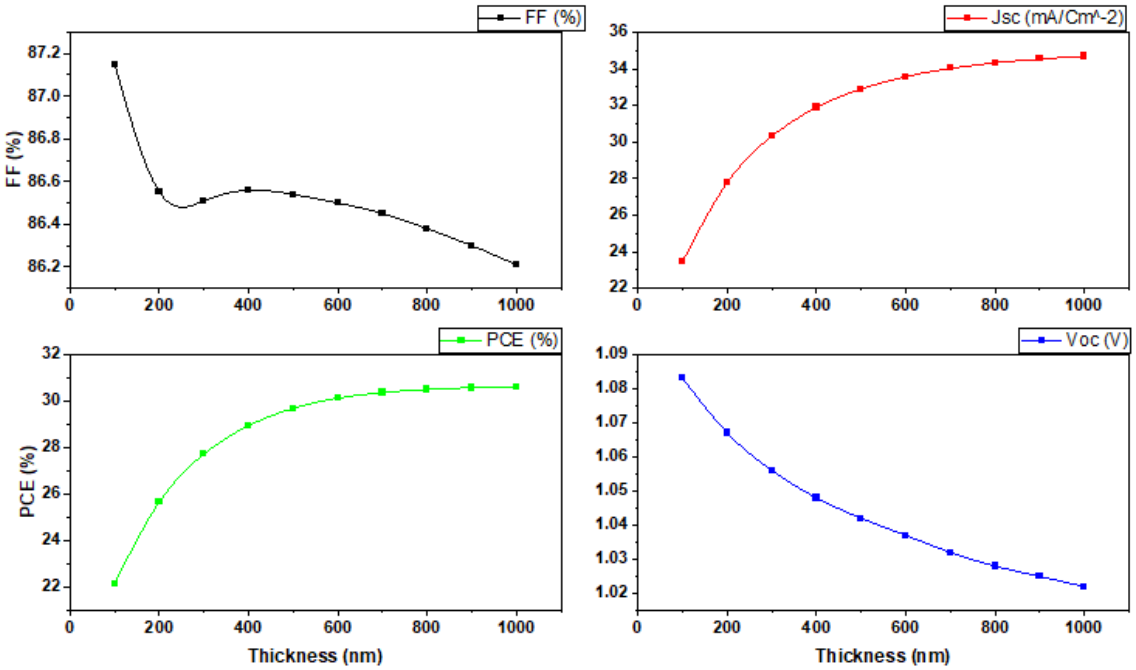

Fig. 2. Photovoltaic output as a function of absorber layer thickness.

3.1.1. ETL and HTL thickness

ETL and HTL thickness was varied from 10 nm to 100 nm in this study. Values of V_{OC}, J_{SC}, FF, and PCE did not change noticeably and became almost saturated at 20nm. ETL and HTL thickness do not have any significant impact on the performance of this device. The effect of ETL and HTL thickness on this PSC has been illustrated in Figure 3.

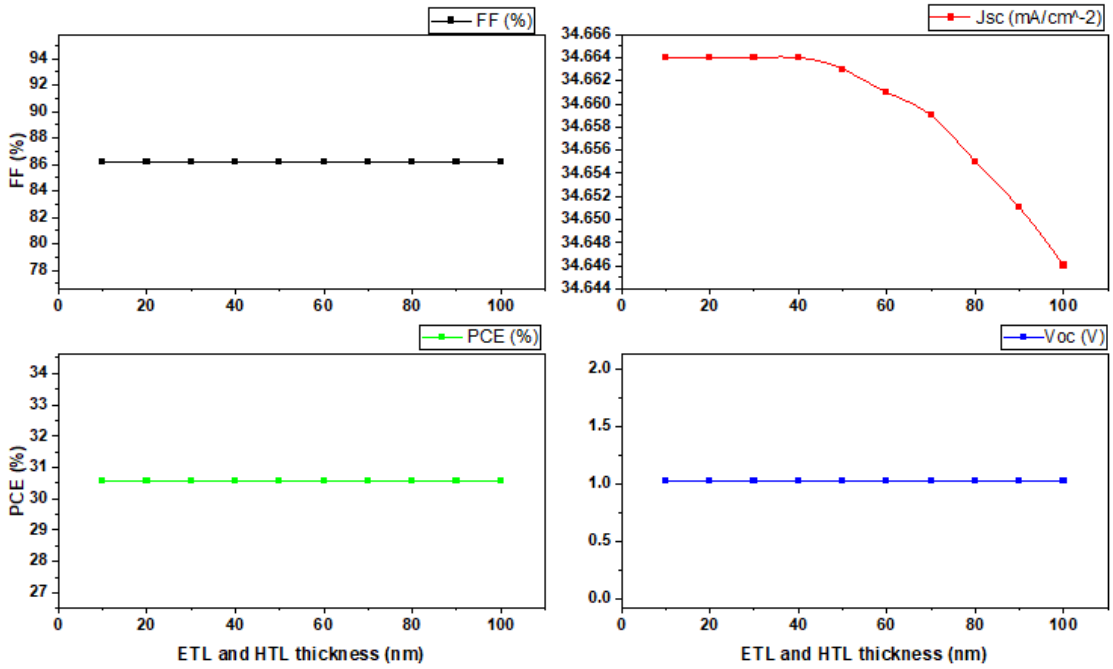

Fig. 3. Photovoltaic output as a function of ETL and HTL thickness.

3.2. Acceptor doping density

One of the most important parameters of perovskite solar cell is acceptor density. $CH_3NH_3S_nI_3$ is very unstable in ambient atmosphere. While exposed to air due to oxidization Sn^{2+} will rapidly oxidize into a more stable form Sn^{4+} [16]. It acts like a P-type dopant within the material in self-doping process and the whole semiconductor acts like p-type. Here SnF_2 is added to prevent the formation of Sn^{2+} to Sn^{4+} [41,42,43]. In this study acceptor density has been varied from 10^{14} Cm^{-3}- 10^{19} Cm^{-3} as per previous studies [16,17]. As acceptor density increases from 10^{14} Cm^{-3}-10^{16} Cm^{-3} V_{OC}, PCE and FF increases. Increase in photogenerated carrier is the reason for increasing PCE and FF. The Highest value of PCE was recorded at 10^{16} Cm^{-3}. The Highest value of FF was recorded at 10^{17} Cm^{-3} and after that FF starts to drop. FF drops because of non-radiative recombination away from open circuit condition and decrease in transport layer mobility, which causes SRH recombination to increase [18]. As acceptor density increases from 10^{14} Cm^{-3}-10^{19} Cm^{-3} , V_{OC} rises and J_{SC} falls. Rise in , V_{OC} is the result of increased radiative recombination at open circuit condition [18,19]. J_{SC} decreases because of an overall increase in recombination in short circuit condition [18]. With the cumulative effect of V_{OC}, J_{SC} and FF according to equation (VI) PCE drops after 10^{16} Cm^{-3}. Change in V_{OC}, J_{SC} FF and PCE are illustrated in figure 4.

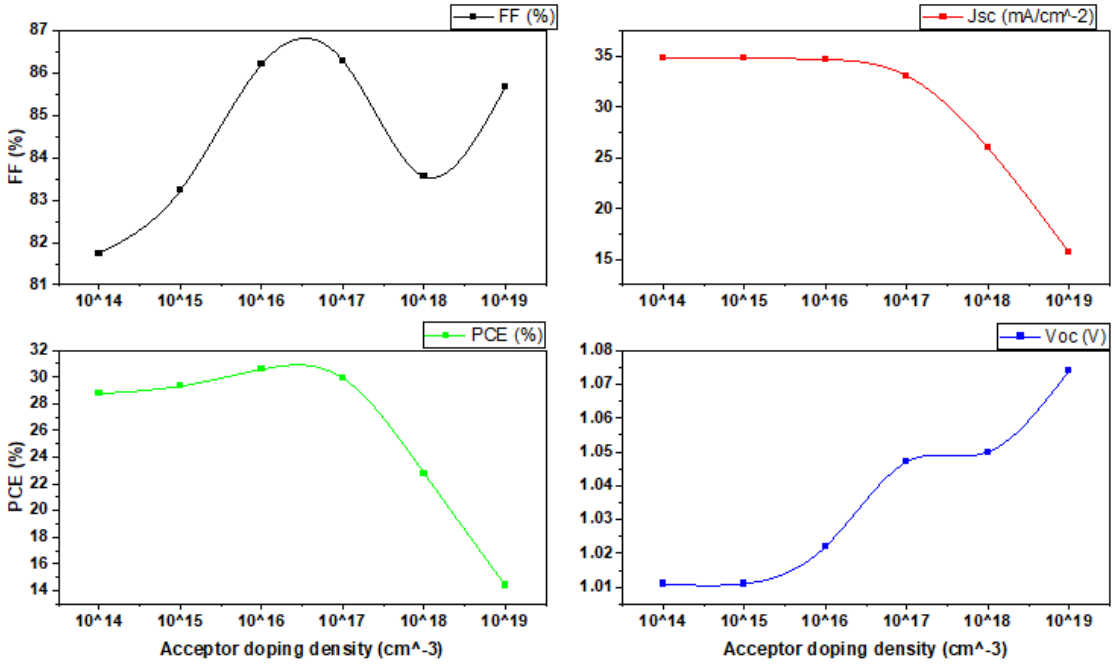

Fig. 4. Photovoltaic output as a function of acceptor doping density

3.3. Defect density

While improving the performance of solar cell, defect density is another crucial parameter that needs to be taken in consideration. Perovskite have a high defect tolerance but still there are some deep defects that hampers the PCE of perovskite to reach Schockley- Queisser limit [20,21]. Defects can cause degradation in device performance by excessive carrier recombination [22]. Most of the defects stays mainly on the surface of perovskite and on grain boundaries [23,24]. Defects also exists in the interface of two different layers of solar cells and they are called interfacial defects. Native point defects are the most studied defects in halide perovskite. Perovskite has vacancies, interstitial, substitutions, dopants and antisite occupancy defects. Higher order defects such as grain boundaries and dislocations also exist in perovskite [25]. Defect density influences the recombination of perovskite specially the Schockley Read Hall (SRH) recombination as in equation (VII) [26]. Shockley Read Hall model for interface defects is given in equation (VIII) [26].

$$SRH = \frac{np - ni^2}{\tau_p(n+n_i\, e^{(Et-Ei)/KT} + \tau_n\,(P+n_i\, e^{(Ei-Et)/KT})} \tag{7}$$

$$SRH_{interface} = \frac{n_{if} \times P_{if} - n_i^2}{\frac{p_{if}+p_1}{S_n} + \frac{n_{if}+n_1}{S_p}} \tag{8}$$

$$n_1 = n_i\, e^{(Et-Ei)/KT} \tag{9}$$

$$p_1 = n_i\, e^{(Ei-Et)/KT} \tag{10}$$

$$\tau_n = \frac{1}{\sigma_n V_{th} N_t} \tag{11}$$

$$\tau_p = \frac{1}{\sigma_p V_{th} N_t} \tag{12}$$

$$S_P = \sigma_p V_{th} N_{ti} \tag{13}$$

$$S_n = \sigma_n V_{th} N_{ti} \tag{14}$$

where,

Symbol	Definition
N	Electron density
P	Hole density
ni^2	Thermal generation
Et	Trap energy level
Nt	Perovskite defect density
τ_n	Lifetime of electron
τ_p	Lifetime of hole
σ_n	Electron capture cross-section
σ_p	Hole capture cross-section
V_{th}	Thermal velocity
S_P	Hole surface recombination velocity
S_n	Electron surface recombination velocity
N_{ti}	Interface defect density
Ei	Intrinsic energy level
KT	Thermal Energy

In this study perovskite defect density has been varied from 10^{18} Cm^{-3} to 10^{14} Cm^{-3} to investigate the effect of defect density on perovskite [10,17,27]. As defect density decreases from 10^{18} Cm^{-3} V_{OC}, J_{SC}, FF. PCE increases. Highest value of V_{OC}, J_{SC}, FF and PCE (1.0225 v, 34.680360 mA/Cm^2, 86.21% and 30.57% respectively) was recorded at 10^{14} Cm^{-3} as shown in figure 6. As defect density decreases recombination reduces because defect works as recombination center in semiconductor devices [10]. Non-radiative recombination also decreases as defect density decreases [28]. In a uniform excitation, electron hole pairs are generated equally but with higher defects free charge carrier gets trapped and that results in reduced carrier life time and shorter carrier diffusion length [29]. Theoretical expression of diffusion length is given below.

$$\text{Carrier diffusion length, } L = \sqrt{D\tau} \tag{15}$$

D= Diffusion co-efficient

$$D = \mu KT/q \tag{16}$$

μ = Carrier mobility.

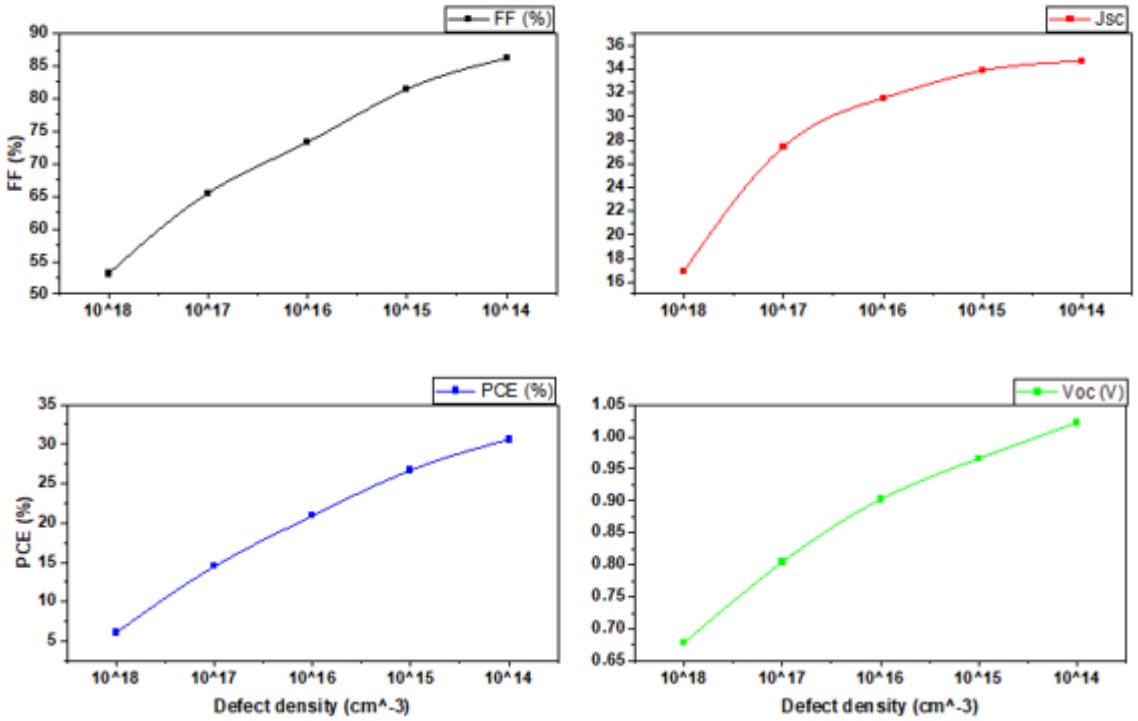

Fig. 5. Effect of defect density on photovoltaic parameters.

3.4. Interface defect

To test the effect of N_{ti} on PCE in ETL / Perovskite interface N_{ti} has been varied from a lower value of $10^{10}Cm^{-3}$ to a higher value of 10^{13} Cm^{-3}. As N_{ti} increases from $10^{10}Cm^{-3}$ PCE starts to drop. PCE drops to 28.94% at $N_{ti}= 10^{13}$ Cm^{-3} as shown in figure 6. Numerical analysis was conducted to check the effect of different values of Et, σ_p and σ_n on PCE for different values N_{ti}(where $N_{ti}= 10^{10}$ Cm^{-3} -10^{13} Cm^{-3}.). For ETL/Perovskite layer it is evident from the figure:6 that Et and σ_n does not have any effect on PCE for highest ($N_{ti}=10^{13}$ Cm^{-3}) to lowest ($N_{ti}=10^{10}$ Cm^{-3}) value of N_{ti} . But for σ_p, PCE drops with decreasing σ_p for all values (Highest to lowest) of Nt. In HTL/Perovskite layer as shown in figure:7 (d) values of Nt have been varied from 10^{10} Cm^{-3}-10^{13} $Cm^{-3}$and a decrease in PCE was observed with increasing Nt. At Nt= 10^{13} Cm^{-3} PCE was 29.56 %. From figure:7 (a), (b) and (c) it can be observed, Et does not have any effect on PCE for any values of Nt. But PCE drops with decreasing σ_n for all values of Nt and PCE drops for σ_p while Nt=10^{12} Cm^{-3} but remains saturated for other values of Nt.

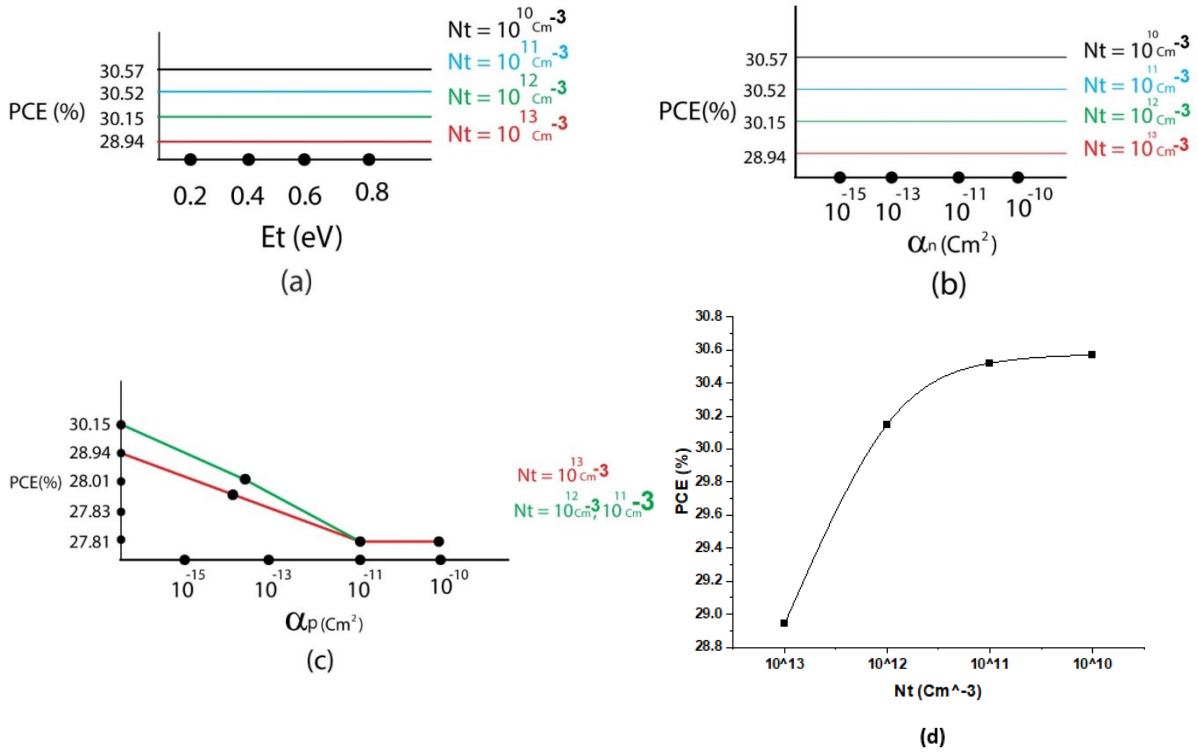

Fig. 6. Effect on PCE for different values of (a) Et (b) σ_n (c) σ_p (d) Nt on ETL / Perovskite interface.

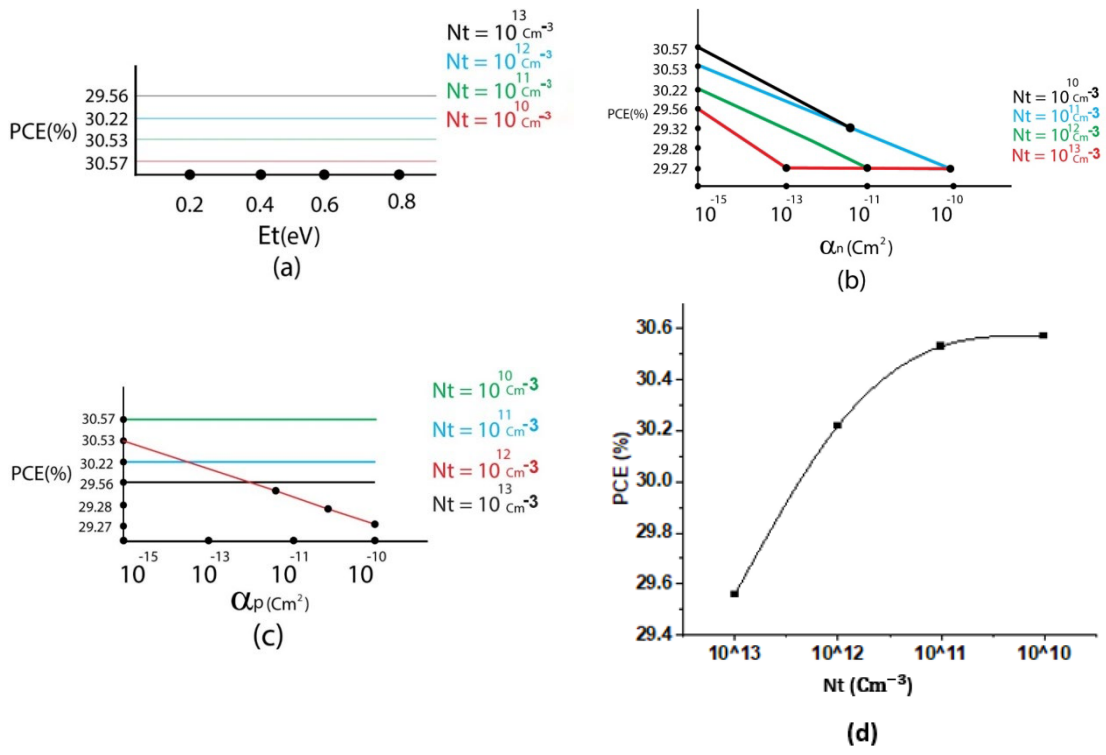

Fig. 7. Effect on PCE for different values of (a) Et (b) σ_n (c) σ_p (d) Nt on HTL / Perovskite interface.

3.5. Metal work function

Metal work function (Ø) is an important parameter to develop a greater built-in voltage V_{bi} [12]. V_{bi} increases for a higher value of Ø. As V_{bi} increases an electric field also increases in the direction of p-n junction. As a result of that increased electric field V_{OC} increases because there is an increase in photogenerated carrier. This overall V_{bi} increase is unidirectional. Such potential is helpful for majority drift within absorber layer towards the junction [30]. PCE and FF increases for a higher value of Ø. This is because Schottky barrier for hole decreases in HTL/Metal contact interface as the value of Ø increases [12]. It helps hole transportation to back contact. J_{SC} has small dependency on Ø comapred to V_{OC}, FF and PCE. Figure 8 illustrates the effect of metal work function on different photovoltaic parameters and figure 9 shows the band diagram of PSC for different anode material.

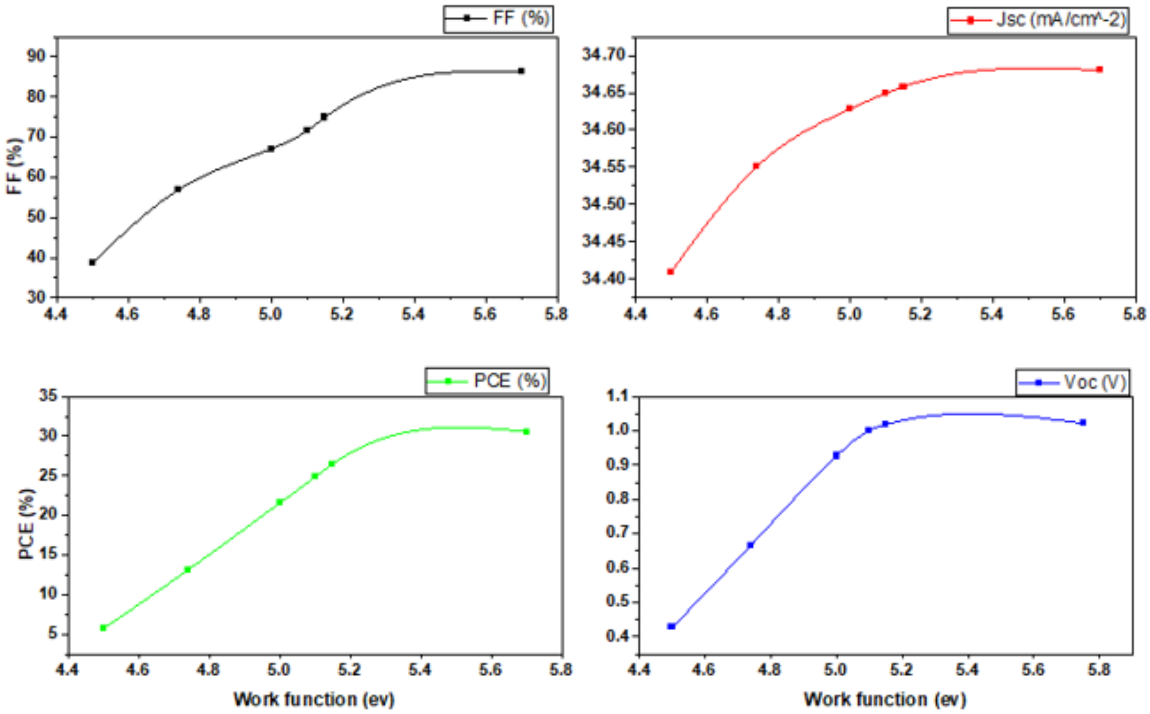

Fig. 8. V_{OC}, J_{SC} and FF, PCE for different metal work function.

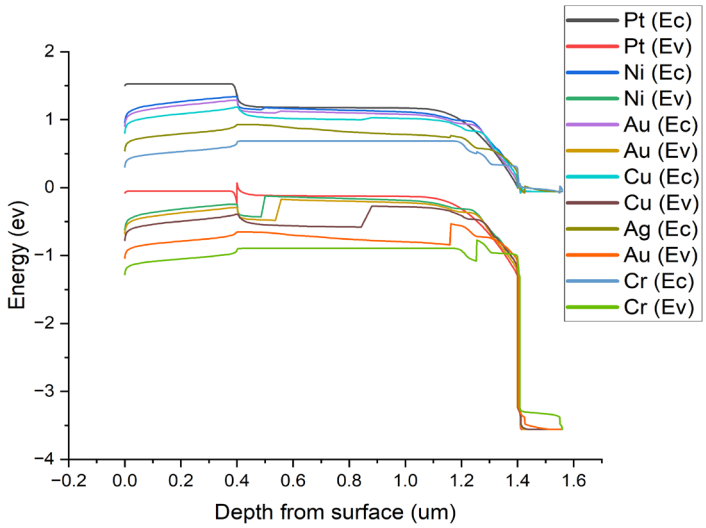

Fig. 9. PSC band diagram for different anode material.

4. Conclusion

In this work the structure FTO/ZnO/$MASnI_3$/$CuSbS_2$/Pt was observed to be a highly efficient eco-friendly PSC. In this study some experiments were conducted on this novel structure to find out the optimum performance of this device. Previous works on PSC have been evaluated and their techniques have been used throughout this study to improve the performance of this PSC. Acceptor density, absorber thickness, defect density, interface defect density, ETL and HTL thickness and metal work function have been varied to achieve the highest performance. Acceptor density was set at 10^{16} Cm^{-3} where this simulation work shows highest efficiency (30.57%). It was found that lower defect density is beneficial for PSC because of lower trap, less recombination center and shorter diffusion length. Perovskite defect density and interface defect density have been kept 10^{14} Cm^{-3} and 10^{10} Cm^{-3} respectively. A balanced absorber thickness is necessary to get highest performance because carrier recombination depends on absorber layer thickness. Absorber thickness is kept at 1000nm. ETL and HTL thickness do not have any noticeable impact on the performance of this device. A high work function is always better because, Schottky barrier decreases with higher work function. In this study Pt ($\emptyset = 5.7ev$) is used as back metal contact. As a future work, This perovskite solar cell can be combined with piezo material for biomedical device for healthcare purpose in [52]-[56].

References

[1] M. Wang, W. Wang, B. Ma, W. Shen, L. Liu, K. Cao, S. Chen, W. Huang, Nanomicro Lett., vol. 13, p. 62, (2021); https://doi.org/10.1007/s40820-020-00578-z.
[2] S. Rahmany, L. Etgar, ACS Energy Lett., vol. 5, pp. 1519–1531, (2020); https://doi.org/10.1021/acsenergylett.0c00417.
[3] A. Babayigit, A. Ethirajan, M. Muller, B. Conings, Nat Mater., vol 15, pp. 247–251, (2016); https://doi.org/10.1038/nmat4572.
[4]L. Meng, J. You, Y. Yang, Nat Commun., vol. 9, pp. 5265, (2018); https://doi.org/10.1038/s41467-018-07255-1.
[5] M. Kumar, A. Raj, A. Kumar, A. Anshul, Opt Mater (Amst)., vol. 108, pp. 110213, (2020); https://doi.org/10.1016/j.optmat.2020.110213.
[6] H. Thanoon, Przegląd Elektrotechniczny., vol 1, pp. 174–177, (2022); https://doi.org/10.15199/48.2022.06.31.
[7] E. Rickus,: Fourth E.C. Photovoltaic Solar Energy Conference, Springer Netherlands, Dordrecht, 1982, pp. 831–835; https://doi.org/10.1007/978-94-009-7898-0_139.
[8] M. Dehghan, A. Behjat, RSC Adv., vol. 9, pp. 20917–20924, (2019); https://doi.org/10.1039/C9RA01839E.
[9] C. Garza, S. Shaji, A. Arato, E. Perez Tijerina, G. Alan Castillo, T.K. Das Roy, B. Krishnan, Solar Energy Materials and Solar Cells vol. 95, pp. 2001–2005, (2011); https://doi.org/10.1016/j.solmat.2010.06.011.
[10] H.-J. Du, W.-C. Wang, J.-Z. Zhu, Chinese Physics B., vol. 25, p. 108802, (2016); https://doi.org/10.1088/1674-1056/25/10/108802.
[11] W. Wang, G. Zhi, J. Liu, L. Hao, L. Yang, Y. Zhao, Y. Hu, Journal of Nanoparticle Research., vol. 22, pp. 294, (2020); https://doi.org/10.1007/s11051-020-05024-0.
[12] L. Lin, L. Jiang, P. Li, B. Fan, Y. Qiu, Journal of Physics and Chemistry of Solids., vol. 124, pp. 205–211,(2019); https://doi.org/10.1016/j.jpcs.2018.09.024.
[13] M. Lazemi, S. Asgharizadeh, S. Bellucci, Physical Chemistry Chemical Physics., vol. 20, pp. 25683–25692, (2018); https://doi.org/10.1039/C8CP03660H.
[14] M. Liu, M.B. Johnston, H.J. Snaith, Nature., vol. 501, pp. 395–398, (2013); https://doi.org/10.1038/nature12509.
[15] L. Lin, L. Jiang, P. Li, B. Fan, Y. Qiu, Journal of Physics and Chemistry of Solids., vol. 124, pp. 205–211, (2019); https://doi.org/10.1016/j.jpcs.2018.09.024.

[16] F. Hao, C.C. Stoumpos, D.H. Cao, R.P.H. Chang, M.G. Kanatzidis, Nat Photonics., vol. 8, pp. 489–494, (2014); https://doi.org/10.1038/nphoton.2014.82.
[17] F. Hao, C.C. Stoumpos, P. Guo, N. Zhou, T.J. Marks, R.P.H. Chang, M.G. Kanatzidis, J Am Chem Soc., vol. 137, pp. 11445–11452, (2015); https://doi.org/10.1021/jacs.5b06658.
[18] B. Das, I. Aguilera, U. Rau, T. Kirchartz, Effect of Doping, Adv Opt Mater., vol. 10, (2022); https://doi.org/10.1002/adom.202101947.
[19] A. Polman, H.A. Atwater, Nat Mater., vol. 11, pp. 174–177, (2012); https://doi.org/10.1038/nmat3263.
[20] M.L. Agiorgousis, Y.-Y. Sun, H. Zeng, S. Zhang, J Am Chem Soc., vol. 136, pp. 14570–14575, (2014); https://doi.org/10.1021/ja5079305.
[21] J. Kim, S.-H. Lee, J.H. Lee, K.-H. Hong, J Phys Chem Lett., vol. 5, pp. 1312–1317, (2014); https://doi.org/10.1021/jz500370k.
[22] L. Vines, E. Monakhov, A. Kuznetsov, J Appl Phys., vol. 132, (2022); https://doi.org/10.1063/5.0127714.
[23] H. Yu, F. Wang, F. Xie, W. Li, J. Chen, N. Zhao, Adv Funct Mater., (2014) n/a-n/a.; https://doi.org/10.1002/adfm.201401872.
[24] C. Ran, J. Xu, W. Gao, C. Huang, S. Dou, Chem Soc Rev., vol. 47, pp. 4581–4610, (2018); https://doi.org/10.1039/C7CS00868F.
[25] Y.M. Lee, I. Maeng, J. Park, M. Song, J.-H. Yun, M.-C. Jung, M. Nakamura, Front Energy Res., vol. 6, (2018); https://doi.org/10.3389/fenrg.2018.00128.
[26] M.S.S. Basyoni, M.M. Salah, M. Mousa, A. Shaker, A. Zekry, M. Abouelatta, M.T. Alshammari, K.A. Al-Dhlan, C. Gontrand, IEEE Access., vol. 9, pp. 130221–130232, (2021); https://doi.org/10.1109/ACCESS.2021.3114383.
[27] T. Minemoto, M. Murata, J Appl Phys., vol. 116, (2014); https://doi.org/10.1063/1.4891982.
[28] D. Luo, R. Su, W. Zhang, Q. Gong, R. Zhu, Nat Rev Mater., vol. 5, pp. 44–60, (2019); https://doi.org/10.1038/s41578-019-0151-y.
[29] A. Sridharan, N.K. Noel, H. Hwang, S. Hafezian, B.P. Rand, S. Kéna-Cohen, Phys Rev Mater., vol. 3, p. 125403, (2019); https://doi.org/10.1103/PhysRevMaterials.3.125403.
[30] A. Kumar, A.D. Thakur, Jpn J Appl Phys., vol. 57, (2018) 08RC05; https://doi.org/10.7567/JJAP.57.08RC05.
[31] V. D'Innocenzo, G. Grancini, M.J.P. Alcocer, A.R.S. Kandada, S.D. Stranks, M.M. Lee, G. Lanzani, H.J. Snaith, A. Petrozza, Nat Commun. 5, p.3586, (2014); https://doi.org/10.1038/ncomms4586.
[32] S.D. Stranks, G.E. Eperon, G. Grancini, C. Menelaou, M.J.P. Alcocer, T. Leijtens, L.M. Herz, A. Petrozza, H.J. Snaith, Science (1979), 342, pp. 341–344, (2013); https://doi.org/10.1126/science.1243982.
[33] J.S. Manser, P. V. Kamat, Nat Photonics. 8, pp. 737–743, (2014); https://doi.org/10.1038/nphoton.2014.171.
[34] T. Baikie, Y. Fang, J.M. Kadro, M. Schreyer, F. Wei, S.G. Mhaisalkar, M. Graetzel, T.J. White, J Mater Chem A Mater. 1, p. 5628, (2013); https://doi.org/10.1039/c3ta10518k
[35] F. Sani, S. Shafie, H. N. Lim, A. O. Musa, Materials vol. 11, no. 6, p. 1008, 2018; https://doi.org/10.3390/ma11061008
[36] M. Caputo, N. Cefarin, A. Radivo, N. Demitri, L. Gigli, J. R. Plaisier, M. Panighel, G. Di Santo, S. Moretti, A. Giglia, M. Polentarutti, F. De Angelis, E. Mosconi, P. Umari, M. Tormen, A. Goldoni, Scientific Reports, vol. 9, no. 1, p. 15159, 2019/10/22 2019; https://doi.org/10.1038/s41598-019- 50108-0
[37] N. Guo, T. Zhang, G. Li, F. Xu, X. Qian, Y. Zhao, Journal of Semiconductors, vol. 38, no. 1, p. 014004, 2017; https://doi.org/10.1088/1674-4926/38/1/014004
[38] D. Liu, Q. Li, J. Hu, H. Jing, K. Wu, Journal of Materials Chemistry C, 10.1039/C8TC04065F vol. 7, no. 2, pp. 371-379, 2019; https://doi.org/10.1039/C8TC04065F
[39] M. Dehghan, A. Behjat, RSC Adv. 9, pp. 20917–20924, 2019 https://doi.org/10.1039/C9RA01839E.
[40] Fadiyah Makin, Firoz Alam, Mark A. Buckingham, David J. Lewis, Scientific Reports, volume 12, p. 5627, 2022; https://doi.org/10.1038/s41598-022-08822-9

[41] H.-J. Du, W.-C. Wang, J.-Z. Zhu, Chinese Physics B. 25, p. 108802 ,2016; https://doi.org/10.1088/1674-1056/25/10/108802
[42] Z. Zhao, F. Gu, Y. Li, W. Sun, S. Ye, H. Rao, Z. Liu, Z. Bian, C. Huang, Advanced Science. 4, 2017; https://doi.org/10.1002/advs.201700204.
[43] L. Ma, F. Hao, C.C. Stoumpos, B.T. Phelan, M.R. Wasielewski, M.G. Kanatzidis, J Am Chem Soc. 138, pp. 14750–14755, 2016; https://doi.org/10.1021/jacs.6b09257
[44] P. K. Patel, "Device simulation of highly efficient eco-friendly CH3NH3SnI3 perovskite solar cell," Scientific Reports, vol. 11, no. 1, pp. 1-11, 2021; https://doi.org/10.1038/s41598-021-82817-w

[45] S. Ahmed, F. Jannat, M. A. K. Khan, and M. A. Alim, "Numerical development of eco-friendly Cs2TiBr6 based perovskite solar cell with all-inorganic charge transport materials via SCAPS1D," Optik, vol. 225, p. 165765, 2021/01/01/ 2021; https://doi.org/10.1016/j.
[46] F. Baig, "Numerical analysis for efficiency enhancement of thin film solar cells," Universitat Politècnica de València, 2019. https://doi.org/10.4995/Thesis/10251/118801
[47] I. Kabir and S. A. Mahmood, "Comparative Study on Perovskite Solar Cells Using Inorganic Transport Layers," in 2019 IEEE International Conference on Telecommunications and Photonics (ICTP), 2019, pp. 1-4; https://doi.org/10.1109/ICTP48844.2019.9041784
[48] Gagandeep, M. Singh, and R. Kumar, "Simulation of perovskite solar cell with graphene as hole transporting material," in AIP Conference Proceedings, 2019, vol. 2115, no. 1, p. 030548: AIP Publishing LLC; https://doi.org/10.1063/1.5113387
[49] Numerical modeling of ultra-thin CuSbS2 heterojunction solar cell with TiO2 electron transport and CuAlO2:Mg BSF layers M. ATOWAR RAHMAN* Department of Electrical and Electronic Engineering, University of Rajshahi, Rajshahi-6205, Bangladesh https://doi.org/10.1364/OME.465498
[50] Device simulation of lead-free MASnI3 solar cell with CuSbS2 (copper antimony sulfide) Chandni Devi1,* and Rajesh Mehra1 1 Department of Electronics and Communication Engineering, National Institute for Technical Teachers Training and Research, Chandigarh, India https://doi.org/10.1007/s10853-018-03265-y
[51] D. Bartesaghi, A. H. Slavney, M. C. Gélvez-Rueda, B. A. Connor, F. C. Grozema, H. I. Karunadasa, and T. J. Savenije, "Charge Carrier Dynamics in Cs2AgBiBr6 Double Perovskite," The Journal of Physical Chemistry C, vol. 122, no. 9, pp. 4809-4816, 2018/03/08 2018; https://doi.org/10.1021/acs.jpcc.8b00572
[52] M. I. Haque, K. Yoshibayashi, J. Wang, G. Fischer, J. Kirchner, “Design and Evaluation of Directional Antenna for Shoe-mounted Sensor for Position Identification of Elderly Wanderer”, Sensing and Bio- Sensing Research, Elsevier, Volume 34, December 2021, 100451 (doi: 10.1016/j.sbsr.2021.100451).
[53] M. I. Haque, K. Yoshibayashi, J. Wang, G. Fischer and J. Kirchner, “Directive Antenna Design at 2.4 GHz on Foot Surface for Wanderer Location Identification,” 2020 International Symposium on Antennas and Propagation (ISAP), 2021, pp. 635-636, (doi: 10.23919/ISAP47053.2021.9391396).
[54] M. I. Haque, R. Yamada, J. Shi, J. Wang, D. Anzai, “Channel Characteristics and Link Budget Analysis for 10-60 MHz Band Implant Communication”, IEICE Transactions on Communications, Apr. 2021, Vol. E 104-B, No.4,410-418 (DOI: 10.1587/transcom.2020EBP3075).
[55] M. I. Haque, R. Yamamoto, J. Wang and K. -I. Kakimoto, “Measurement Performance of NKN Piezo Material for Powering Shoe- mounted Sensor,” 2022 International Conference on Innovations in Science, Engineering and Technology (ICISET), 2022, pp. 324-328, (doi: 10.1109/ICISET54810.2022.9775861).
[56] M. I. Haque, J. Wang, D. Anzai, “Path Loss and Group Delay Analysis at 10-60 MHz Human Body Communication Band”, IEICE Technical Report, EMCJ2019-78,13th Dec 2019,19-22.